

16th International Conference on Greenhouse Gas Control Technologies, GHGT-16

23rd -27th October 2022, Lyon, France

Novel Analytical Mass Transfer Model for CO₂ Capture using Sprays

Awan Bhati*, Serhat Bilyaz and Vaibhav Bahadur

Walker Department of Mechanical Engineering, The University of Texas at Austin, Austin, TX

Abstract

The capture of carbon dioxide from the earth's atmosphere has become very important in order to fight the climate crisis and meet the Paris agreement by 2050. Basic solutions such as amines, NaOH, etc., are used as absorbent liquids to capture CO2 from flue gas or atmospheric air. The goal of such carbon capture plants is to obtain the utmost CO2 removal rate, which is limited by the overall effective area between the absorbent and gas flow. Spray systems are expected to increase the mass transfer between the sprayed liquid and its surrounding gas environment by increasing the overall effective area between the liquid and the gas. The mass transfer in a spray-based channel is strongly dependent on design parameters such as nozzle specifications, channel specifications, gas flow rate, solvent flow rate, temperature, pressure, and thermophysical parameters of the solvent and the gas. The overall mass transfer (K_GA_V) is a crucial design indicator to evaluate the system's effectiveness. This study develops a novel analytical model to predict mass transfer in spray-based systems for CO₂ capture by evaluating K_GA_V and capture efficiency. The model considers the Sauter Mean Diameter (SMD) as the uniform droplet diameter of the spray across the entire channel height, solvent properties of 30 wt% monoethanolamine (MEA), channel dimensions, nozzle orifice diameter, temperature, total gas pressure, CO₂ partial pressure, liquid flow rate, and gas flow rate as input parameters. The model predictions are then validated across different experimental studies for a range of design parameters, such as the liquid flow rate, inlet solvent loading, etc. The relative importance of the incorporation of equilibrium partial pressure of $CO_2(P^*)$ into amine with respect to CO_2 partial pressure is also investigated. It is found that its effect on K_GA_V is prominent in high liquid flow rate and low inlet solvent loading regimes where the overall CO₂ capture is high. Lastly, the variation of key parameters such as K_GA_V , K_G , A_V , α , X_{CO_2} along the channel height is studied, which gives insights towards the optimization of the channel height for a new CO₂ capture system at given operating conditions.

Keywords: Carbon capture; overall mass transfer; absorbents; capture efficiency; solvent loading; flue gas; effective surface area.

Nomenclature	
A_d	Area of single droplet (m ²)
A_{v}	Effective mass transfer cross-sectional area (m ² /m ³)
C_{init}	Initial concentration of MEA (kmol/m ³)
d	Droplet diameter (μm)
D	Diameter of the channel (m)

^{*} Corresponding author. Email address: bhati137@utexas.edu

GHGT-16 A. Bhati et. al.

2

 $D_{CO_2,g}$ Diffusivity of CO₂ in gas phase (m²/s) $D_{CO_2,MEA}$ Diffusivity of CO₂ in liquid phase (m²/s)

 G_I Inert gas flow rate (m³/m²-h)

 $H_{CO_2,MEA}$ Henry's constant for solubility of CO₂ in amine (kPa-m³/kmol)

H Height of the channel (m)

J Flux of CO_2 absorption (kmol/m²-h)

 K_G Total mass transfer coefficient (kmol/m²-h-kPa) k_g Mass transfer coefficient of gas phase (kmol/m²-h-kPa)

k_L Reactive mass transfer coefficient of liquid phase (kmol/m²-h-kPa)

k₂ Second-order reaction rate constant (m³/mol-s) n_{CO_2} Mole flow rate of CO₂ consumed (mol/s)

 $n_{MEA,free}$ Moles of free amine in solvent $n_{CO_2,cons}$ Moles of CO₂ consumed

 n_{tot} Total mole flow rate of gas (mol/s) N Number of droplets per unit length (m⁻¹)

 n_d Number of droplets

 P_{CO_2} Partial pressure of CO_2 in gas phase (kPa)

P* Equilibrium CO₂ partial pressure at given CO₂ loading and temperature

 P_{tot} Total operating pressure (kPa)

 \dot{Q}_G Gas flow rate (m³/s)

 Q_G Flux of gas flow rate (m³/m²-h)

 \dot{Q}_L Liquid flow rate (m³/s)

 Q_L " Flux of liquid flow rate (m³/m²-h)

R Universal gas constant (= 8.314 kJ/kmol-K)

T Temperature (K)

UVelocity of single droplet (m/s) V_d Volume of single droplet (m³) X_{CO_2} Mole fraction of CO_2 in gas stream

 $X_{CO_2,in}$ Mole fraction of CO₂ in gas stream at inlet $X_{CO_2,out}$ Mole fraction of CO₂ in gas stream at exit Y_{CO_2} Mole ratio of CO₂ to N₂ in gas stream

z Distance along channel (m)

Greek Characters

 α Solvent loading (mole CO_2 / mole solvent)

 α_{in} Solvent loading at liquid inlet υ_g Gas dynamic viscosity (kg/m-s)

n Capture efficiency (%)

Parameter defined for simplification of equations (= $\alpha/(1+\alpha)$)

1. Introduction

As per the World Health Organization, the biggest threat to humanity has been climate change. The increased release of CO₂ into the environment by burning of fossil fuels to generate electricity is the primary source of anthropogenic climate change [1]. To tackle this challenge, the United Nations formed the Paris agreement which aims for net-zero CO₂ emission by the year 2050. The current operational Carbon Capture and Storage (CCS) capacity

is around 40Mt per annum which must increase at last 100-fold by 2050 to meet the Paris agreement. Thus, the need for CCS has become imminent. Such a technology would need to be adapted at the power plants where CO₂ is emitted, also called as point-source capture. In order to achieve net-zero CO₂ emissions, there would also be a need to capture CO₂ directly from air, also called as Direct Air Capture (DAC) [2].

A typical CO₂ capture plant, whether it be from a point-source capture or direct air capture, comprises of an absorber, and a stripper [2, 3]. The absorber allows for CO₂ capture using solid or liquid sorbents and convert it into salts. Monoethanolamine (MEA), methyldiethanolamine (MDEA), diethanolamine (DEA), sodium-hydroxide (NaOH), Calcium oxide (CaO), etc. are some of the materials used for CO₂ capture [4-8]. Gas absorption from an aqueous alkanolamine solution is the most well-established technology for CO₂ capture [9]. The CO₂ loaded solvents are passed into the stripper where they are heated to remove CO2 and the solvent can be reused. The absorber is designed to attain maximum CO₂ capture by enhancing contact area and thus mass transfer between the liquid solvent and CO₂ rich gas stream. This can be attained by packed beds or spray-based system [7, 10, 11]. A packed bed allows solvent breakdown into thin films as it hits the packing bead material, which leads to increased contact area. The packing arrangement can be randomly arranged, structured, or be a hybrid. The material can be metal, ceramic, or plastic. Three primary mass transfer properties, the effective area (a_e) , gas mass transfer coefficient (k_g) , and liquid mass transfer coefficient (k_L) were studied for random and structured packing [12]. The effective area was found to increase with liquid flow rate until it hits an asymptote at the packing material surface area which is generally around 100-300 m²/m³. The gas and liquid side mass transfer coefficients were strong functions of gas and liquid velocities respectively. Several models have been developed to obtain these three parameters for a packed bed, some of which have been reviewed in [13].

A typical spray-based capture system consists of a nozzle at the top of the reactor which allows for atomization of liquid solvent into smaller droplets. This causes an increase in effective contact area between the liquid and gas streams. The gas stream can be co-current or counter-current. The inlet conditions of both liquid and gas streams are known, and the outlet conditions are experimentally or numerically obtained. A spray system removes the need of extra material that a packing bed would require. Furthermore, a spray system also allows for visualization of the absorber better which wouldn't be as easily possible on a packed bed. However, there are only limited studies on CO₂ capture using spray-based systems [10]. Some such studies are outlined in Table 1.

Reference	Inlet CO ₂ Composition	Solvent Used	Key Finding
[7, 8]	5-15 vol%	MEA	Performance of spray found to be 2-7 times higher than packing
[2]	Air	NaOH	The cost of CO ₂ capture ranges between 53-127 \$/ton-CO ₂ .
[14]	2.5 vol%	NaOH	Swirling inlet gas flow increases K_GA_v by 31-49%
[6]	12 mol%	NaOH	K_GA_v was obtained at two different height within the channel
[15]	10-20 kPa	NH_3	Highest K_GA_v appears for 15kPa and gas temperature 30-40 °C
[16]	15 vol%	MEA	Variation along column height was studied
[17]	8-18 vol%	MEA	Diameter varying reactor used for experiments and simulations
[18]	15 vol%	$NH_3 + PZ$	Upward and downward liquid injection was compared

Table 1. A summary of studies on spray-based CO₂ capture.

An experimental study was conducted using MEA to compare the two methods of area enhancement [7, 8]. A spray-based reactor using three different nozzles was compared with Mellapak 500Y packing. They found that the system's performance was heavily dependent on the liquid flow rate and the spray system was 2-7 times higher in performance than packing. A technoeconomic analysis for different channel height and liquid flow rates to ascertain the feasibility of using NaOH to capture CO₂ from air using sprays was conducted [2]. The cost of CO₂ capture in absorber was in the range 53-127 \$/ton-CO₂. This excluded costs in the stripper for solvent recovery and CO₂ sequestration. It was found that the equivalence ratio of NaOH to CO₂ is the key parameter affecting CO₂ removal

efficiency [5]. The effect of a swirling inlet gas flow on the overall mass transfer coefficient (K_GA_V) was also studied and a 31-49% enhancement with respect to axial inlet gas flow was observed [14]. A roughly 30% variation in the Sauter Mean Diameter (SMD) along radial distance within the channel was reported [19]. Parameters such as K_GA_{ν} , SMD and planar surface area were experimentally evaluated at two different heights within the channel and along radial distance, for different flow rates and inlet loading conditions [6]. It was found that the inlet loading did not affect planar surface area significantly, but the K_GA_V was heavily dependent on the inlet loading. A numerical study was conducted to study the flow within a single droplet and a vortex was found within the droplet enhancing mixing between fresh solvent and solvent that has captured CO₂ [20]. An experimental study with NH₃ was conducted and K_GA_V was observed to increase with NH₃ concentration, liquid to gas flow rate, and gas flow rate [15]. The highest $K_G A_v$ was found for inlet gas flow condition of 15kPa CO₂ partial pressure and temperature of 30-40°C. Another experimental study using three spray columns connected in series was conducted to obtain the variation of solvent loading and CO₂ concentration along channel height [16]. They also studied the effect of solvent loading and temperature on solvent properties and overall CO₂ removal rate of the system. A diameter varying reactor along with dual nozzle impinging MEA from two sides was studied using both experiments and ANSYS simulations [17]. They found the system to have doubled the overall effective area when compared to the traditional single nozzle spray tower. An air-blast atomizing column using MEA and NaOH as solvents was studied and MEA was found to obtain better overall performance [21]. Thermophysical properties of solvent blends of NH₃ and piperazine (PZ) blends were experimentally evaluated [18]. This was utilized in an ANSYS model and the upward and downward liquid injection was compared. It was found that upward injection increased droplet residence time thus improving overall mass transfer and CO₂ capture.

It should be noted that the solvent used for the studies listed in Table 1 is limited to MEA, NaOH and NH₃. There is a need to conduct more experimental studies with other solvents and solvent blends to get a better understanding of spray-based CO₂ capture. Furthermore, all of the previously reported modeling work validates with experiments conducted by the same group. No study exists till date that develops a model that validates spray-based CO₂ capture systems from different studies, and can thus be used for the development of a new CO₂ capture plant. The previous modeling works are either completely empirical in nature which requires experimentation, or are ANSYS simulations which require high computing power. This work focusses on an analytical model that is validated with experiments on 30wt% MEA used in a spray-based CO₂ capture absorber from [6] and [8]. The presented model can be numerically solved much faster than an ANSYS simulation. The work outlines a novel approach to modelling, thus creating a good baseline for future development of the model. It provides key insights into the system's performance within the channel, which gives information on the performance at a given operating condition and a given reactor size. This information can be used to obtain ideal operating conditions and reactor design. This also helps with developing a new capture plant as the techno-economic analysis to develop a plant would be heavily dependent on the size of the reactor.

2. Mathematical Model

A typical spray-based capture plant is shown in Figure 1. Lean solvent is introduced from the top (z = 0) via a spray. The lean solvent can be fresh ($\alpha_{in} = 0$) or CO₂ loaded ($\alpha_{in} > 0$). After capturing CO₂, the rich solvent exits from the bottom of the channel (z = H). The CO₂ rich gas stream ($Y_{CO_2,in}$) is introduced from the bottom and the CO₂ lean gas stream exits the top ($Y_{CO_2,out}$). Any system is operated at a known inlet gas stream and solvent loading conditions, along with other operating parameters like \dot{Q}_L , \dot{Q}_G , P_{tot} , T, etc. Using these operating parameters, the variation of Y_{CO_2} and α within the reactor has been evaluated. Equation 1 can be used to estimate flux of CO₂ absorption [14].

$$J = K_G(P_{CO_2} - P^*) (1)$$

Here, P_{CO_2} is partial pressure of CO₂ in gas stream and P^* is equilibrium partial pressure of CO₂ for a given amine loading and temperature which can be obtained from equation 2 [22]. K_G is the overall mass transfer coefficient which

is obtained according to the two-film theory from both gas-side and liquid-side mass transfer coefficient as described in equation 3 below [23]. The gas side mass transfer coefficient (k_g) is obtained from Sherwood number correlation for a falling droplet in countercurrent flow. The reactive liquid side mass transfer coefficient (k_L) incorporates both reaction kinetics and mass transfer boundary layer.

$$P^* = \exp(39.3 - 12155 / T - 19\alpha^2 + 1105\alpha / T + 12800\alpha^2 / T)$$
 (2)

$$\frac{1}{K_G} = \frac{1}{k_g} + \frac{1}{k_L} \tag{3}$$

The two mass transfer coefficients can be obtained from the equations below [23], where C_{init} is the concentration of amine at the inlet, $D_{CO_2,MEA}$ is the diffusivity of CO₂ in the amine solution, $D_{CO_2,g}$ is the diffusivity of CO₂ in the gas stream, and H_{CO_2} is the Henry's constant for solubility of CO₂ in amine solution.

$$k_{g} = \left(\frac{D_{CO_{2},g}}{RTd}\right) \left(2 + 0.552 * \left(\frac{Ud}{v_{g}}\right)^{0.5} \left(\frac{v_{g}}{D_{CO_{2},g}}\right)^{\frac{1}{3}}\right)$$
(4)

$$k_{L} = \frac{\sqrt{k_{2}C_{init}(1 - 2\alpha)D_{CO_{2},MEA}}}{H_{CO_{2}}}$$
 (5)

Here, k_2 is second-order reaction rate constant for 30wt% MEA solution which can be obtained from empirical relations provided in [24].

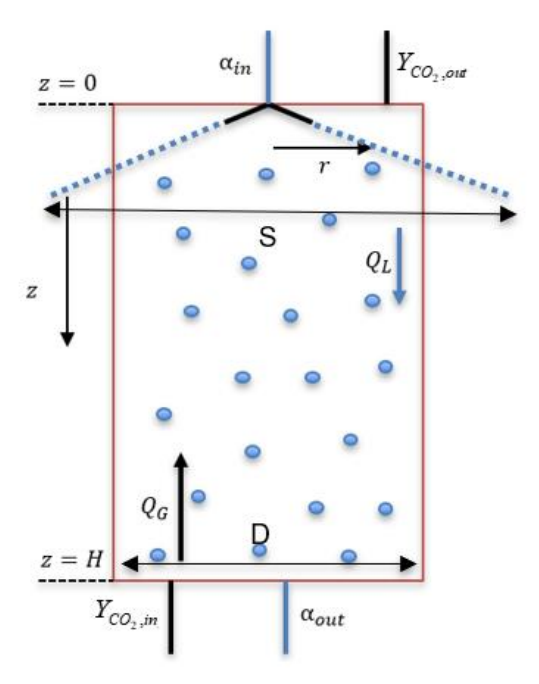


Fig. 1. Schematic of a typical spray-based CO₂ absorber.

Next, a parameter N is defined as the number of droplets per unit length as shown below in equation 6. This parameter describes droplet density and can be evaluated in terms of droplet size, velocity and liquid flow rate as described in equation 7 where the factor f estimates the fraction of liquid in the form of droplets. It is considered to be equal to 1 when the spread associated with the spray (S) is smaller than the channel diameter (D), and is equal to D/S when D<S. The spread of the spray (S) is obtained from correlations provided in [25].

$$N = \frac{dn_d}{dz} \tag{6}$$

$$N = \frac{Q_L}{v_d V_d} f \tag{7}$$

This gives the rate of moles of CO₂ captured per unit distance as shown in equation 8.

$$\frac{d \, n_{CO_2}}{dz} = JNA_d \tag{8}$$

The rate of moles of CO₂ captured can also be expressed as $dn_{CO_2} = n_{N_2} dY_{CO_2}$ where $n_{N_2} = \frac{Q_{N_2}}{P_{tot}RT}$. Substituting into equation 8, and rearranging, the variation of mole ratio of CO₂ along column height can be expressed as shown in equation 9 below.

$$\frac{dY_{CO_2}}{dz} = K_G RT \frac{\dot{Q_L}}{Q_{N_2}} \frac{A_d}{UV_d} \left(\frac{Y_{CO_2}}{1 + Y_{CO_2}} - \frac{P^*}{P_{tot}} \right)$$
(9)

For the liquid side, the change in loading of solvent can be described by equation 10. The rate of absorption of CO₂ into the liquid is the same as the rate at which CO₂ is removed from the gas phase as shown in equation 11.

$$\alpha = \frac{n_{CO_2,init} + n_{CO_2,cons}}{n_{MEA,init}} = \alpha_{in} + \frac{n_{CO_2,cons}}{n_{MEA,init}}$$
(10)

$$\frac{d \left| n_{CO_2} \right|_{in,liq}}{dz} = \frac{d \left| n_{CO_2} \right|_{out,gas}}{dz} \tag{11}$$

The rate of moles of CO₂ consumed in the liquid phase can also be expressed as $dn_{CO_2}|_{liq} = \dot{Q}_L C_{init} d\alpha$. Upon applying this relation with equations 8 and 9, and rearranging, the variation of amine loading along distance can be obtained as described in equation 12 below.

$$\frac{d\alpha}{dz} = \frac{P_{tot}}{C_{init}} \frac{6}{Ud} K_G \left(\frac{Y_{CO_2}}{1 + Y_{CO_2}} - \frac{P^*}{P_{tot}} \right)$$
 (12)

To solve the given set of differential equations for Y_{CO_2} and α , the gas properties are obtained for flue gas with given inlet CO₂ concentration. The liquid properties such as $D_{CO_2,MEA}$ and $H_{CO_2,MEA}$ are obtained using the N_2O

analogy wherein the properties are measured for CO_2 and N_2O in water, and then for N_2O in amine. The ratio of property values for CO_2 and N_2O in water, along with those of N_2O in amine is used to obtain the properties of CO_2 in amine as directly measuring the properties of CO_2 in amine becomes challenging due to its reactivity. The detailed procedure for the same is described in [26], which provides these relations as functions of temperature. The velocity of the droplet was evaluated using stokes flow for a droplet with initial velocity obtained from jet velocity, and gas properties from given inlet CO_2 concentration of gas. The velocity was found to reach terminal velocity within first 20% of the channel height.

Equations 9 and 12 can be used to evaluate α and Y_{CO_2} along column height. For a given operating condition, α_{in} and $Y_{CO_2,in}$ are known. The two equations were solved as initial value problems (IVP) with solve_ivp function of the scipy library in Python using a relative tolerance of 10^{-6} . The predictor-corrector method was used to solve the two IVPs. At first, an initial guess of $Y_{CO_2,out}$ was used along with the given inlet loading. The velocity profile, liquid flow rate, gas flow rate, and temperature was used to obtain the parameter $K_G(z)$ in equations 9 and 12. The final solution of the IVP evaluated $Y_{CO_2}(@z = H) = Y_{CO_2,in,pred}$ which is also given for any operating system. The iterated $Y_{CO_2,in}$ was compared with the given $Y_{CO_2,in}$ and the residual was minimized to 10^{-5} using the minimize function in scipy library. Once the residual was minimized, the final profiles for $K_G(z)$, $Y_{CO_2}(z)$ and $\alpha(z)$ was obtained. These were used to obtain overall volumetric mass transfer performance and capture efficiency of the system as-

$$K_{G}A_{v} = \left(\frac{G_{I}}{P_{tot}X_{CO_{2}} - P^{*}}\right) \left(\frac{dY_{CO_{2}}}{dz}\right)$$
(13)

$$\eta(\%) = \frac{X_{CO_2,in} - X_{CO_2,out}}{X_{CO_2,in}} 100 \tag{14}$$

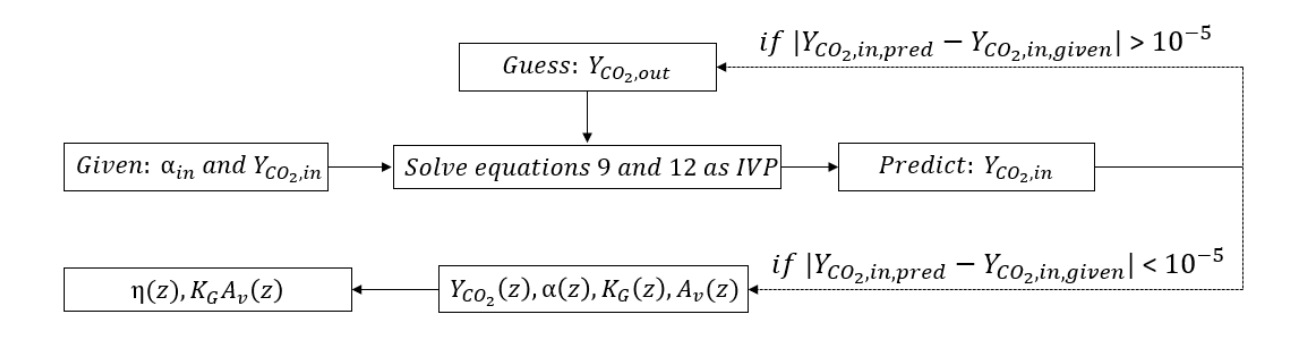


Fig. 2. Block diagram outlining the procedure for solving the system of equations in the model.

The model can be used to study the effect of all relevant design parameters on the overall performance of the system. It also allows us to understand the variation of performance parameters such as K_G and A_V along the channel height. Furthermore, it can be used to understand the effect of P^* on a given system by neglecting it or not. However, it should be noted that the methodology adapted for the model has the following assumptions-

- The droplet-droplet interaction was neglected. The liquid flow was assumed to be spread out into equally sized droplets with the diameter equal to the Sauter mean diameter that was obtained from the manufacturer's data for a given nozzle. Due to the lack of manufacturer's data about nozzle specifications, the droplet-droplet interaction could not be modeled.
- The temperature variation along column height was neglected. The temperature was assumed to be a

GHGT-16 A. Bhati et. al.

constant equal to the temperature at inlet conditions. This was to simplify the model and an extension to this study would be to incorporate the energy equation to the current model and has been left as an exercise for future work.

- The evaporation of amine and water was ignored. The incorporation of evaporation to the model is also left as scope of future work.
- Only variation in axial direction was considered and the model was lumped in the radial direction since D<<H.

3. Results and Discussion

3.1. Validation of the Model

The analytical model was validated with the experimental data from [6] and [8]. Both the studies utilize 30 wt% MEA in a spray column at atmospheric pressure with a nozzle on top of the column and gas stream flowing countercurrent to the liquid flow. The variation in overall performance of the system (K_GA_v) was studied with varying liquid flow rates, inlet solvent loading, and inlet partial pressure of CO₂. The key experimental parameters for the two studies are listed in Table 2 below.

Inlet CO₂ Gas Flow Rate Liquid Flow Rate Inlet solvent Reference Channel Channel Nozzle used Temperature Diameter Height Composition (m^3/m^2-h) (m^3/m^2-h) loading BETE MPL 30 °C [6] 0.2 m 3.7 m 12 mol% 609.8 1.41, 2.12 0 - 0.38 0.30N[8] BETE P-20, 25 °C 382 - 764 1.9 - 10.30 - 0.450.1 m 0.55 m5-15 kPa P-28

Table 2. Relevant parameters for experiments conducted in [6] and [8].

The purely analytical model was validated with the results in [6] and it was observed that the trends in K_GA_v with inlet loading were well-predicted as shown in figure 3. Model was found to perform well for the higher liquid flow rate and was found to underpredict for lower liquid flow rate. This was attributed to the fact that for lower liquid flow rate, the droplet residence time was also low since the Sauter mean diameter was high. Since the droplet-droplet interaction was neglected, the further breakdown of droplets was not considered, thus limiting the predicted K_GA_v . The analytical model also underpredicts for lower inlet loading conditions. This was because any formation of liquid films on the channel walls was neglected, and its contribution to K_GA_v would be much more prominent in lower solvent loading conditions. To circumvent these limitations, slope and bias correction fitting factors were added to the analytical model as described in equation 15 below. Upon the addition of fitting parameters, the trends were in much more agreement with the experiments.

$$K_G A_{v_i}|_{GI} = m * K_G A_{v_i}|_{analytical} + c \tag{15}$$

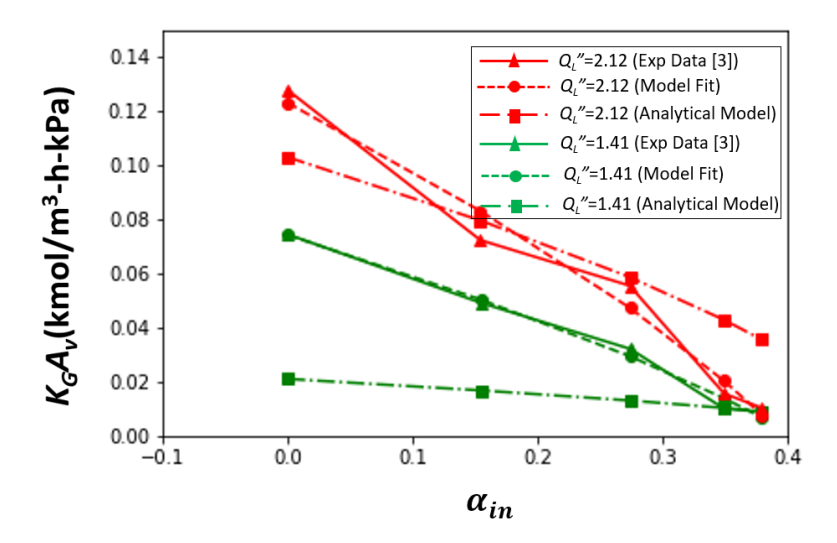


Fig. 3: Model validation across variation in α_{in} for MPL 0.30 N nozzle and two different liquid flow rates used in [6]

Next, the variation with liquid flow rate was studied and the model's performance for experiments in [8] is depicted in figure 4. For the corresponding experiments, inlet CO₂ partial pressure of 15kPa was used along with the P-28 nozzle. It was found to validate within 15% error margin with the experimental data, with significant errors only in region of high liquid flow rate and low solvent loading due to the same reasons mentioned before. Using the model's fit, the optimal operating conditions can be evaluated for P-28 nozzle, given inlet CO₂ partial pressure, and design parameters.

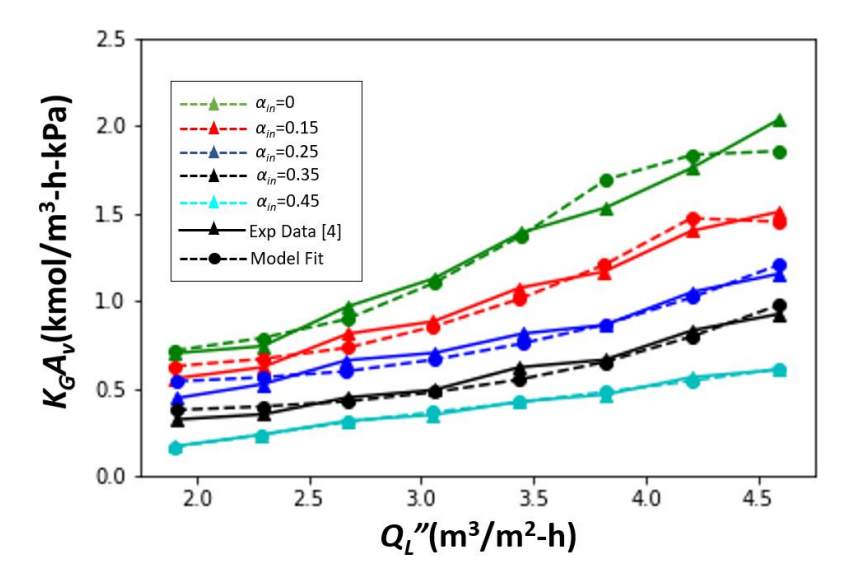


Fig. 4: Validation across variation in Q_L for P-28 nozzle and range of inlet loading used in [8]

Lastly, the model was validated with a range of inlet CO_2 partial pressures and solvent loading conditions from data in [8]. The corresponding experiments were conducted with P-20 nozzle, liquid flow rate of 1.53 m³/m²-h, and gas flow rate of 382-764 m³/m²-h. The model predicted the trends extremely well as can be seen in figure 5. This means that the model predictions can be extrapolated to estimate the system's performance at other operating

conditions such as those in Direct Air Capture where the CO₂ partial pressures are much lower. This also helps identify the ideal operating conditions for the given system.

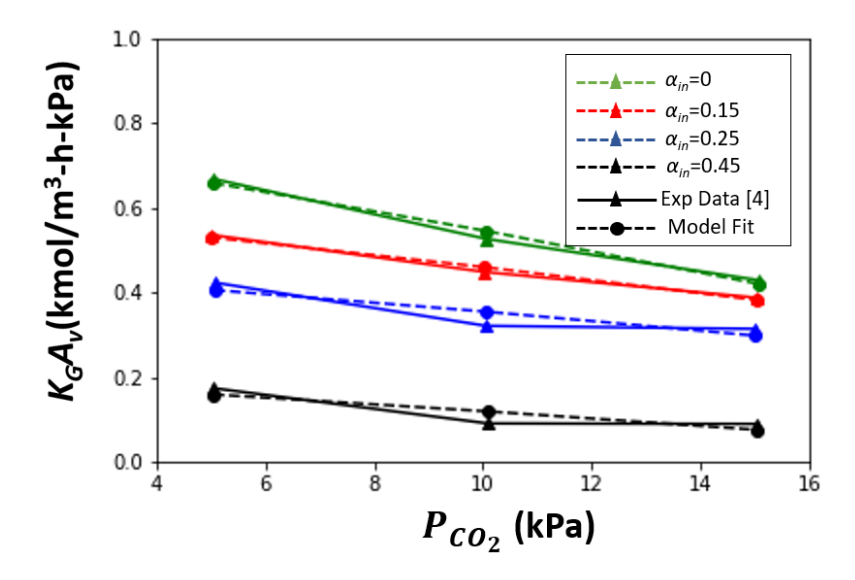


Fig. 5: Validation across variation in $P_{CO_2}(kPa)$ for P-20 nozzle and range of inlet loading used in [8]

3.2. Inferences obtained from the Model

The effect of considering the equilibrium partial pressure of CO_2 on the overall mass transfer has been shown in Figure 6. The purely analytical results were considered with the inclusion and exclusion of P^* to understand its relative importance for a range of inlet loading and liquid flow rates. It was observed that the effect is prominent only for higher flowrates and at lower CO_2 loading, where the overall mass transfer coefficient is high. This was because the driving force $P_{CO_2} - P^*$ is small enough only when the overall removal is high causing P_{CO_2} to be comparable to P^* . In the scenario when overall removal is low due to lower overall mass transfer coefficient, then $P_{CO_2} >> P^*$ and thus the effect of P^* is negligible, which was observed with low liquid flow rates and high CO_2 loading.

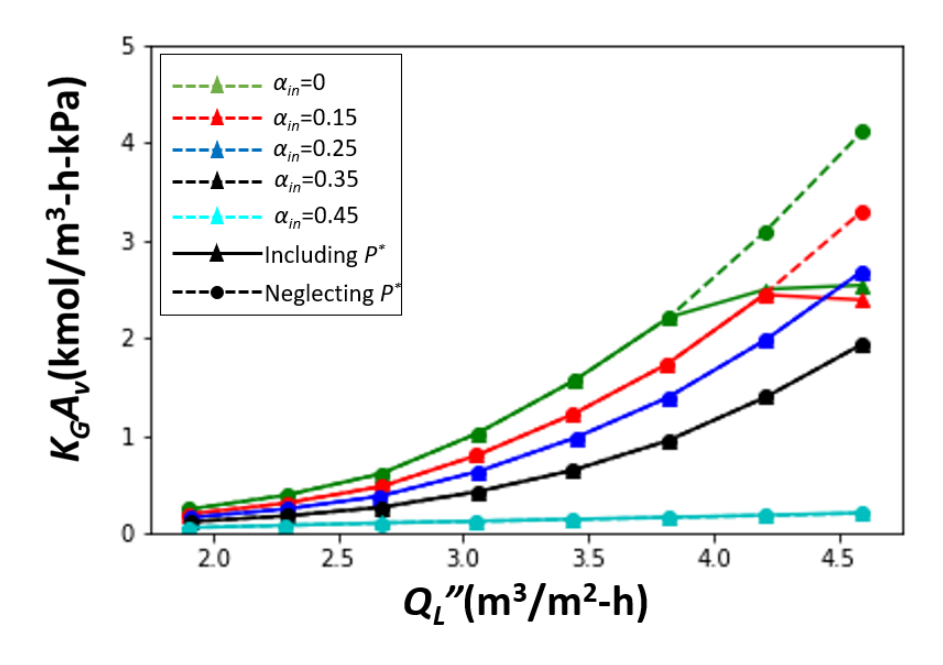


Fig. 6. Effect of inclusion/exclusion of P^* on the model

To obtain further insights from the model, two sets of cases were studied in greater detail. For the first case, the experimental data from [6] and the model's validation was considered. This was corresponding to an inlet loading of 0, 0.15, and a flux of liquid flow rate equal to 1.41 and 2.12 m³/m²-h. The other case studied was the model's validation for experimental data of [8] for P-28 nozzle, flux of liquid flow rate of 3.05 m³/m²-h, and flux of gas flow rate of 382 m³/m²-h. The model was used to obtain variation of mole fraction (X_{CO_2}) , CO₂ loading (α) , volumetric overall mas transfer coefficient (K_GA_v) , total mass transfer coefficient (K_G) , and volumetric effective area (A_v) , along channel height. The results for the same are depicted in figures 7-9, with subfigures (a) and (b) corresponding to the two cases respectively. From figure 7a, it can be shown from the flat lines until the middle of the reactor that the majority of CO₂ consumption takes place in the second half of the reactor for all the four conditions shown. This is not true for the other case when the channel height is only 0.55 m compared to 3.7 m. For the smaller reactor, the consumption takes place throughout the channel. This implies that for the given parametric space in operating conditions, the channel in case b could use an addition to its height while the one in case a is already beyond what's needed. Fig 8a describes the very low K_GA_V in the first half of the reactor followed by a peak around the middle of the channel, while figure 8b shows a steady decrease in the K_GA_V with a peak only at the beginning of the reactor. The overall K_GA_V and K_G were used to obtain A_V along channel height and the results are described in figure 9. It is found that the K_G plateaus in second half of the reactor for the first case with a maximum at the middle of the channel, and A_v reduces along the channel height. For case b, the K_G follows similar trends as $K_G A_v$ and the effective area was again found to behave similar to case a. Figure 9 also shows that the effective area changes significantly with increase in liquid flow rate. It is also found to change only slightly with loading, but this can be attributed to the fact that the way it is evaluated is using $K_G A_V$ and K_G which vary significantly along channel height and inlet loading. The volumetric effective area was found to be in the range 225-425 m²/m³, which was found to be close to the range of 100-300 m²/m³ reported in [7].

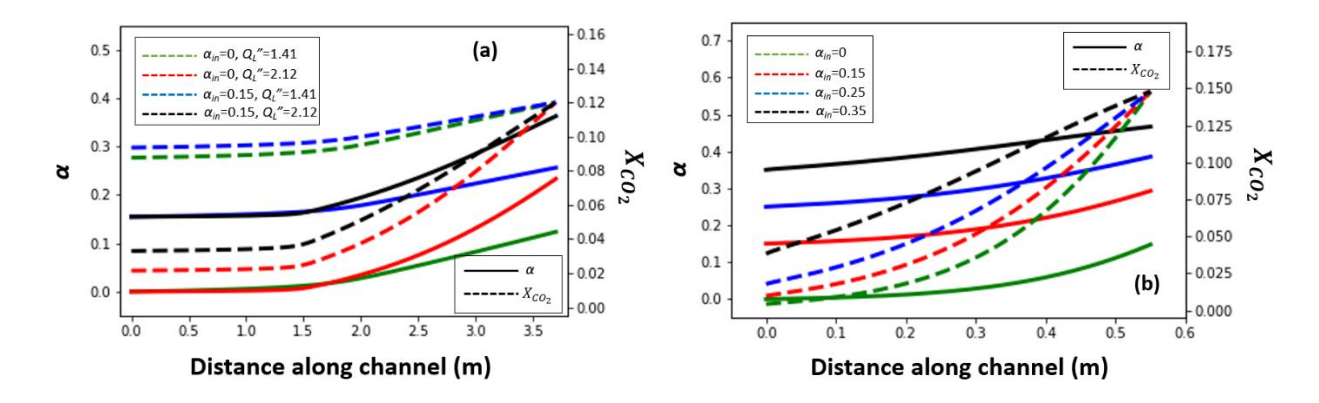


Fig. 7. Variation of α (solid line, left axis) and X_{CO2} (dashed line, right axis) along channel height using model's validation for (a) [6] and (b) [8]

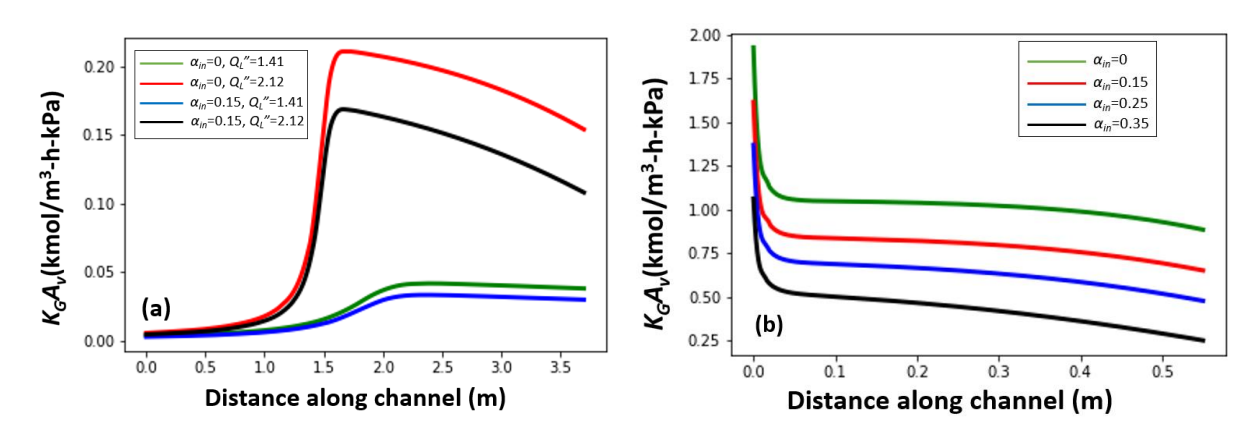


Fig. 8. Variation of $K_G A_v$ along channel height using model's validation for (a) [6] and (b) [8]

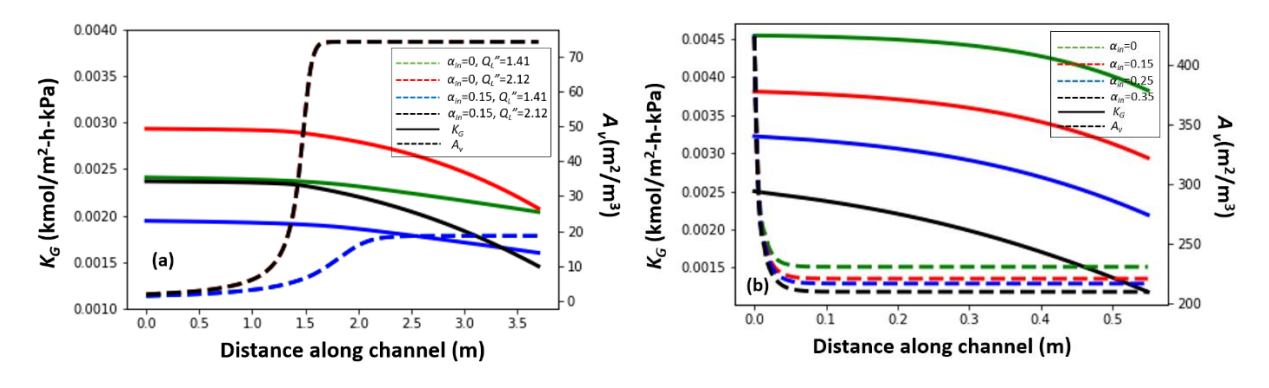


Fig. 9. Variation of K_G (solid line, left axis) and A_v (dashed line, right axis) along channel height using model's validation for (a) [6] and (b) [7, 8]

4. Conclusions

The present work developed a novel analytical model for spray-based CO_2 capture systems. The model was validated for a range of design parameters with experimental data from previous studies. The effect of inclusion of P^*

on the computed performance (K_GA_v) was also studied and was found to be significant only at high liquid flow rate and low solvent loading, which correspond to high overall CO₂ capture. The variation of key parameters such as K_GA_v , K_G , A_v , α , X_{CO_2} along the channel height was studied and it was found that in some cases only parts of the channel are utilized for CO₂ capture. This gives insights into the design of a reactor for given operating conditions. The model can be used to obtain K_GA_v for operating conditions in a wider range than those conducted in the experiments. This data can then be used to obtain the optimum flow conditions for a given system to optimize parameters like CO₂ capture rate, moles of CO₂ captured per total energy consumed [moles/kW], the amount of CO₂ captured by the amount of solvent used [kg-CO₂/kg-solvent], and the amount of CO₂ captured per operating cost [kg-CO₂/\$], based on the designer's needs. Such a study is left as scope of future work.

Acknowledgements

The authors would like to acknowledge fellow lab members Peter Mathews, Mark Hamalian, Karey Maynor, Yasmin Bibi, Palash Acharya and Aritra Kar for their continued support during the course of the project. They would also like to acknowledge grant NSF CBET 1605789 for the financial support.

References

- [1] S. Garg, G. Murshid, F. S. Mjalli, A. Ali, and W. Ahmad, "Experimental and correlation study of selected physical properties of aqueous blends of potassium sarcosinate and 2-piperidineethanol as a solvent for CO2 capture," *Chem. Eng. Res. Des.*, vol. 118, pp. 121–130, 2017, doi: 10.1016/j.cherd.2016.12.013.
- [2] J. K. Stolaroff, D. W. Keith, and G. V. Lowry, "Carbon dioxide capture from atmospheric air using sodium hydroxide spray," *Environ. Sci. Technol.*, vol. 42, no. 8, pp. 2728–2735, 2008, doi: 10.1021/es702607w.
- [3] S. F. Yates, A. Bershitsky, and R. J. Kamire, "A Closed-Loop CO 2 and Humidity Recovery System for Deep Space Missions," 47th Int. Conf. Environ. Syst., no. July 16-20, pp. 1–16, 2017.
- [4] J. C. Chen, G. C. Fang, J. T. Tang, and L. P. Liu, "Removal of carbon dioxide by a spray dryer," *Chemosphere*, vol. 59, no. 1, pp. 99–105, 2005, doi: 10.1016/j.chemosphere.2004.09.076.
- [5] Z. Niu, Y. Guo, and W. Lin, "Experimental studies on CO2 capture in a spray scrubber using NaOH solution," in 2009 International Conference on Energy and Environment Technology, ICEET 2009, 2009, vol. 3, pp. 52–55, doi: 10.1109/ICEET.2009.479.
- [6] Y. Tamhankar *et al.*, "Spray absorption of CO2 into monoethanolamine: Mass transfer coefficients, dropsize, and planar surface area," *Chem. Eng. Res. Des.*, vol. 104, pp. 376–389, 2015, doi: 10.1016/j.cherd.2015.08.012.
- [7] J. Kuntz and A. Aroonwilas, "Performance of spray column for CO2 capture application," *Ind. Eng. Chem. Res.*, vol. 47, no. 1, pp. 145–153, 2008, doi: 10.1021/ie0617021.
- [8] J. Kuntz and A. Aroonwilas, "Mass-transfer efficiency of a spray column for CO2 capture by MEA," in Energy Procedia, 2009, vol. 1, no. 1, pp. 205–209, doi: 10.1016/j.egypro.2009.01.029.
- [9] J. Davison, P. Freund, and A. Smith, "Putting carbon back into our soils," *IEA Greenh. Gas R&D Program.*
- [10] N. K. Yeh and G. T. Rochelle, "Liquid-phase mass transfer in spray contactors," *AIChE J.*, vol. 49, no. 9, pp. 2363–2373, 2003, doi: 10.1002/aic.690490912.
- [11] D. Demontigny, P. Tontiwachwuthikul, and A. Chakma, "Comparing the absorption performance of packed columns and membrane contactors," *Ind. Eng. Chem. Res.*, vol. 44, no. 15, pp. 5726–5732, 2005, doi: 10.1021/ie040264k.
- [12] C. Wang, M. Perry, G. T. Rochelle, and A. F. Seibert, "Packing characterization: Mass transfer properties," *Energy Procedia*, vol. 23, pp. 23–32, 2012, doi: 10.1016/j.egypro.2012.06.037.
- [13] D. Flagiello, A. Parisi, A. Lancia, and F. Di Natale, "A review on gas-liquid mass transfer coefficients in packed-bed columns," ChemEngineering, vol. 5, no. 3, 2021, doi: 10.3390/chemengineering5030043.
- [14] K. H. Javed, T. Mahmud, and E. Purba, "The CO2 capture performance of a high-intensity vortex spray scrubber," *Chem. Eng. J.*, vol. 162, no. 2, pp. 448–456, 2010, doi: 10.1016/j.cej.2010.03.038.
- [15] S. Ma, B. Zang, H. Song, G. Chen, and J. Yang, "Research on mass transfer of CO2 absorption using ammonia solution in spray tower," *Int. J. Heat Mass Transf.*, vol. 67, pp. 696–703, 2013, doi: 10.1016/j.ijheatmasstransfer.2013.08.090.
- [16] S. Zimmermann, M. O. Schmid, B. Klein, and G. Scheffknecht, "Experimental Studies on Spray Absorption with the Post Combustion CO2 Capture Pilot-Plant CASPAR," in *Energy Procedia*, 2017, vol. 114, no. November 2016, pp. 1325–1333, doi: 10.1016/j.egypro.2017.03.1252.
- [17] X. M. Wu, Z. Qin, Y. S. Yu, and Z. X. Zhang, "Experimental and numerical study on CO2 absorption mass transfer enhancement for a diameter-varying spray tower," *Appl. Energy*, vol. 225, no. April, pp. 367–379, 2018, doi: 10.1016/j.apenergy.2018.04.053.
- [18] Y. Xu, X. Chen, Y. Zhao, and B. Jin, "Modeling and analysis of CO2 capture by aqueous ammonia + piperazine blended solution in a spray column," Sep. Purif. Technol., vol. 267, no. March, p. 118655, 2021, doi: 10.1016/j.seppur.2021.118655.
- Y. Tamhankar, B. King, R. Whiteley, M. Resetarits, T. Cai, and C. Aichele, "Aqueous amine spray absorption and droplet distribution data for CO2 capture applications," in *Energy Procedia*, 2014, vol. 63, pp. 293–300, doi: 10.1016/j.egypro.2014.11.032.
- [20] W. H. Chen, M. H. Tsai, and C. I. Hung, "Numerical prediction of CO2 capture process by a single droplet in alkaline spray," *Appl. Energy*, vol. 109, pp. 125–134, 2013, doi: 10.1016/j.apenergy.2013.03.082.

GHGT-16 A. Bhati et. al.

- Z. Li, X. Ji, Z. Yang, and X. Lu, "Experimental studies of air-blast atomization on the CO2 capture with aqueous alkali solutions," [21] Chinese J. Chem. Eng., vol. 27, no. 10, pp. 2390–2396, 2019, doi: 10.1016/j.cjche.2019.01.021.
- Q. Xu and G. Rochelle, "Total pressure and CO2 solubility at high temperature in aqueous amines," Energy Procedia, vol. 4, pp. 117-[22] 124, 2011, doi: 10.1016/j.egypro.2011.01.031.
- R. Ramezani, I. M. Bernhardsen, R. Di Felice, and H. K. Knuutila, "Physical properties and reaction kinetics of CO2 absorption into [23] unloaded and CO2 loaded viscous monoethanolamine (MEA) solution," *J. Mol. Liq.*, vol. 329, p. 115569, 2021, doi: 10.1016/j.molliq.2021.115569.
- G. F. Versteeg, L. A. J. Van Dijck, and W. P. M. Van Swaaij, "On the kinetics between CO2 and alkanolamines both in aqueous and [24] non-aqueous solutions. An overview," Chem. Eng. Commun., vol. 144, no. May 2012, pp. 133–158, 1996, doi: 10.1080/00986449608936450.
- [25] Y. Lim, M. Choi, K. Han, M. Yi, and J. Lee, "Performance characteristics of CO2 capture using aqueous ammonia in a single-nozzle spray tower," *Ind. Eng. Chem. Res.*, vol. 52, no. 43, pp. 15131–15137, 2013, doi: 10.1021/ie401981u.

 J. J. Ko, T. C. Tsai, C. Y. Lin, H. M. Wang, and M. H. Li, "Diffusivity of nitrous oxide in aqueous alkanolamine solutions," *J. Chem.*
- [26] Eng. Data, vol. 46, no. 1, pp. 160–165, 2001, doi: 10.1021/je000138x.

16TH GREENHOUSE GAS CONTROL TECHNOLOGIES CONFERENCE

23 - 27 OCTOBER 2022









NOVEL ANALYTICAL MASS TRANSFER MODEL FOR CO, CAPTURE **USING SPRAYS**

Awan Bhati, Serhat Bilyaz and Vaibhav Bahadur

Walker Department of Mechanical Engineering, The University of Texas at Austin, Austin, TX

BACKGROUND AND MOTIVATION

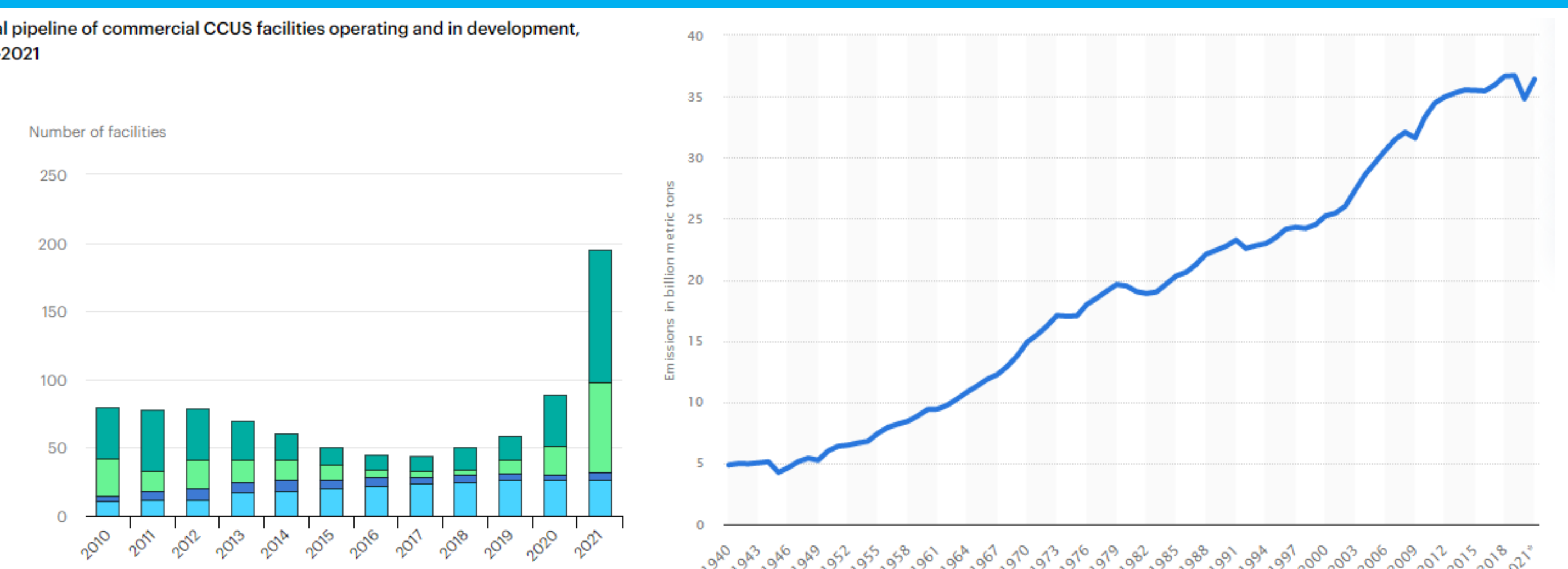


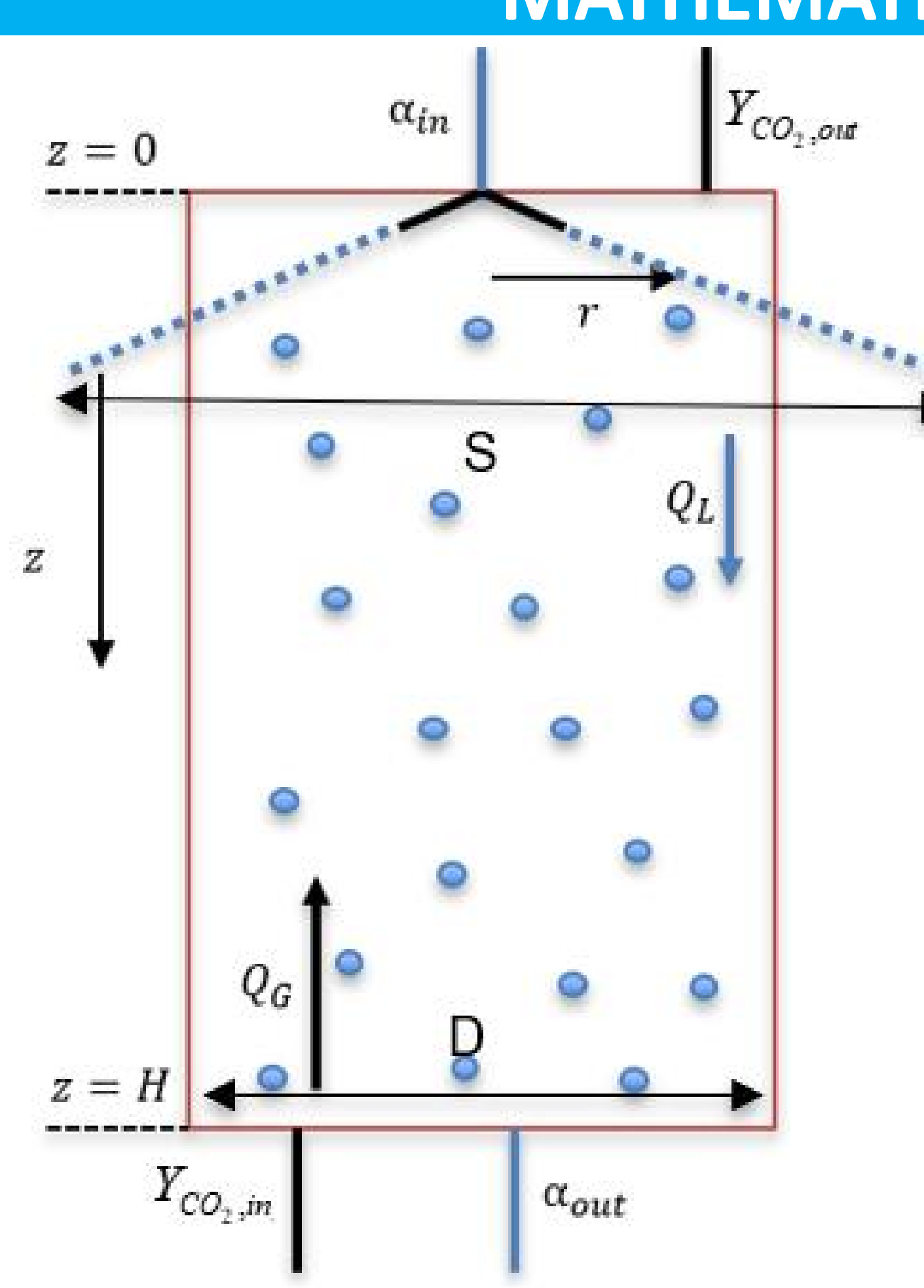
Figure 2: Rising CO₂ emissions per year for the last 80 years [2] Figure 1: Number of CCUS facilities in last decade [1]

- Paris agreement by UN aims at net-zero CO₂ emission by the year 2050.
- Rapid increase in the deployed CCUS facilities to meet the target.
- CO₂ absorber consists of a packed bed, or a spray-based system, or both.
- Lack of models that predict system's performance to design a new capture system.

OBJECTIVES OF CURRENT WORK

- Develop an analytical model that can be validated across different studies [3,4].
- Use model to gain insights on behavior within the reactor.
- Study other potential uses of the validated model.

MATHEMATICAL MODEL



Key Nomenclature:

Effective mass transfer area

Initial concentration of solvent Fraction of liquid in droplet form Flux of CO₂ absorption K_G Total mass transfer coefficient $\dot{n_{CO_2}}$ Mole flow rate of CO₂ consumed $n_{CO_2,cons}$ Moles of CO_2 consumed $n_{MEA,init}$ Moles of amine solvent in solution Number of droplets per unit length \dot{Q}_G Gas flow rate \dot{Q}_L Liquid flow rate \dot{Q}_{N_2} Flow rate of inert gas (N₂) Spread of the spray Velocity of single droplet

 Y_{CO_2} Mole ratio of CO₂ to N₂ in gas stream Solvent loading (mole CO₂ / mole α

Figure 3: Domain for model describing Spray-

based capture plant **Gas-side Equations**

$$J = K_G(P_{CO_2} - P^*)$$

$$N = \frac{dn_d}{dz} = \frac{\dot{Q}_L}{UV_d}f; \quad f = \frac{D}{S}if \ D < S$$

$$\frac{d\dot{n}_{CO_2}|_{gas}}{dz} = JNA_d$$

$$d\dot{n}_{CO_2} = \dot{n}_{N_2}dY_{CO_2} = \left(\frac{P_{tot}\dot{Q}_{N_2}}{RT}\right)dY_{CO_2}$$

Liquid-side Equations

solvent)

Gas-side Equations
$$J = K_{G}(P_{CO_{2}} - P^{*})$$

$$M = \frac{dn_{d}}{dz} = \frac{\dot{Q}_{L}}{UV_{d}}f; \quad f = \frac{D}{S}if \quad D < S$$

$$\frac{d\dot{n}_{CO_{2}}|_{liq}}{dz} = \frac{d\dot{n}_{CO_{2}}|_{gas}}{dz}$$

$$\alpha = \frac{n_{CO_{2},init} + n_{CO_{2},cons}}{n_{MEA,init}} = \alpha_{in} + \frac{n_{CO_{2},cons}}{n_{MEA,init}}$$

$$\frac{d\dot{n}_{CO_{2}}|_{gas}}{dz} = JNA_{d}$$

$$d\dot{n}_{CO_{2}}|_{liq} = \dot{Q}_{L}C_{init}d(\alpha)$$

$$d\dot{n}_{CO_{2}} = \dot{n}_{N_{2}}dY_{CO_{2}} = \left(\frac{P_{tot}\dot{Q}_{N_{2}}}{RT}\right)dY_{CO_{2}}$$

$$\frac{P_{tot}\dot{Q}_{N_{2}}}{RT\dot{Q}_{L}C_{init}}\frac{dY_{CO_{2}}}{dz} = \frac{d\alpha}{dz}$$

$$\frac{dY_{CO_{2}}}{dz} = K_{G}RT\frac{\dot{Q}_{L}}{\dot{Q}_{N_{2}}}\frac{A_{d}}{UV_{d}}\left(\frac{Y_{CO_{2}}}{1 + Y_{CO_{2}}} - \frac{P^{*}}{P_{tot}}\right) \quad (A)$$

$$\frac{d\alpha}{dz} = \frac{P_{tot}}{C_{init}}\frac{6}{Ud}K_{G}\left(\frac{Y_{CO_{2}}}{1 + Y_{CO_{2}}} - \frac{P^{*}}{P_{tot}}\right) \quad (B)$$

- Equations A and B were solved as IVP using the predictor corrector method.
- The residual between predicted and given $Y_{CO_2,in}$ was minimized to 10^{-5} .
- Stokes flow relations were used to obtain velocity profile and thus residence time.
- Liquid properties of 30 wt% MEA were used.
- Analytical model results were fitted with slope and bias correction factors.

$$K_G A_v = \left(\frac{Q_{N_2}}{P_{tot} \left(\frac{Y_{CO_2}}{1 + Y_{CO_2}}\right) - P^*}\right) \left(\frac{dY_{CO_2}}{dz}\right)$$

$$K_G A_v|_{fit} = m * K_G A_v|_{analytical} + c$$

Key assumptions involved in the model:

- The droplet-droplet interaction was neglected.
- Energy equation was not considered, i.e., temperature was assumed a constant.
- The evaporation of amine and water was estimated to be negligible.
- System was lumped in radial direction.

RESULTS

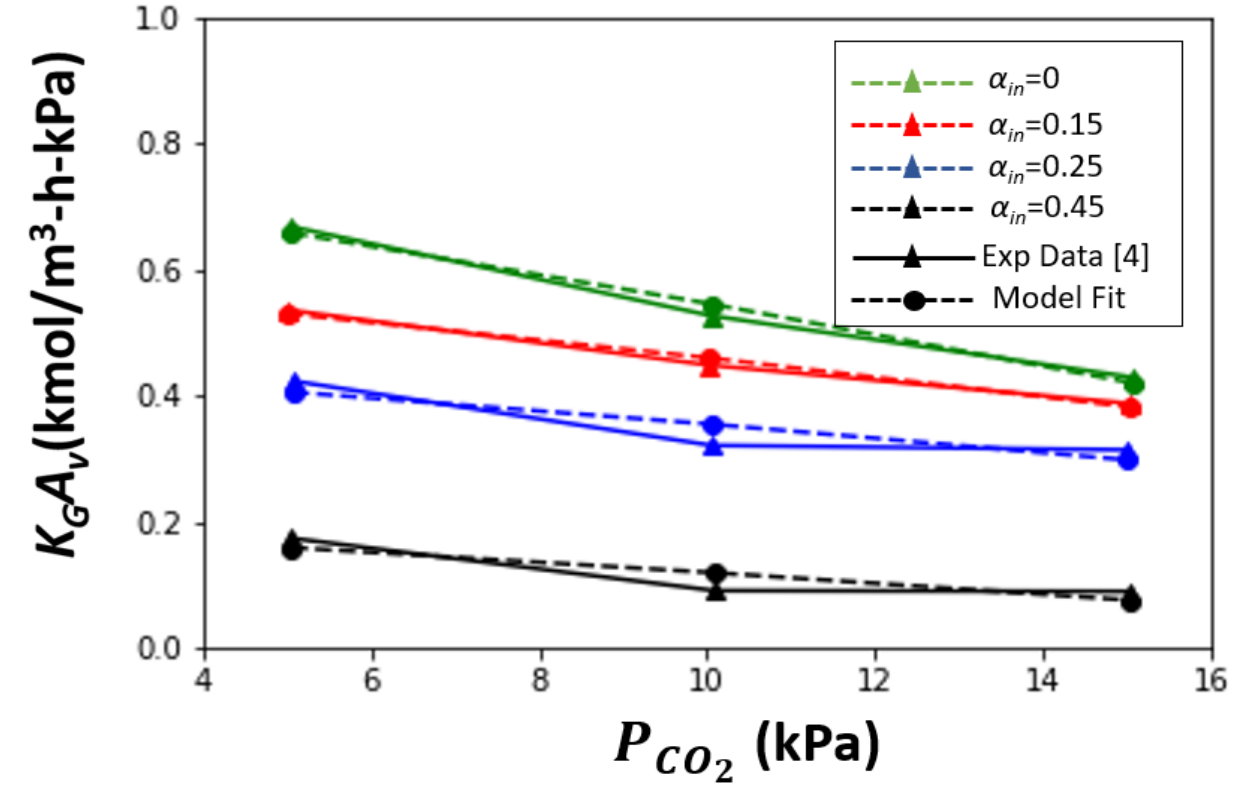
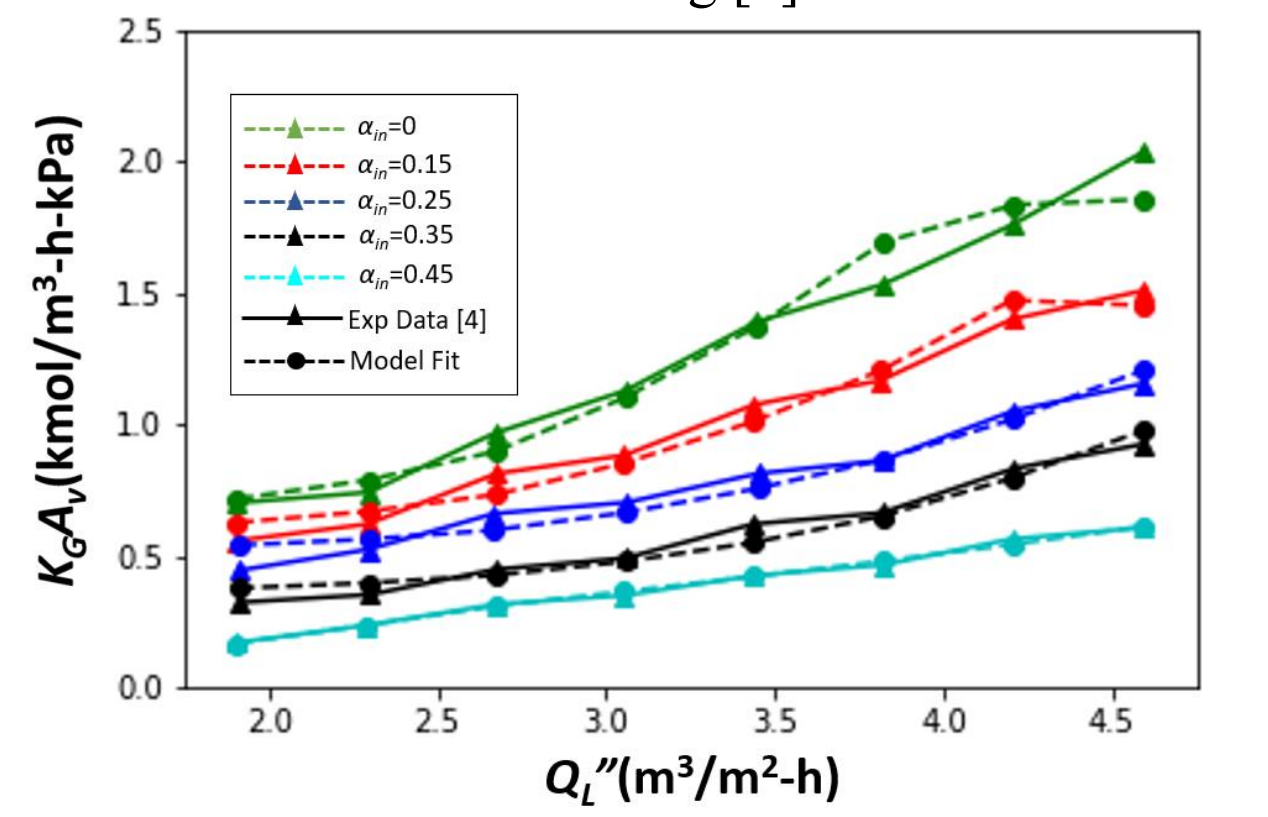


Figure 4: Model validation for variation in K_GA_v with inlet loading [3]

Figure 5: Model validation for variation in K_GA_v with inlet CO₂ partial pressure [4]



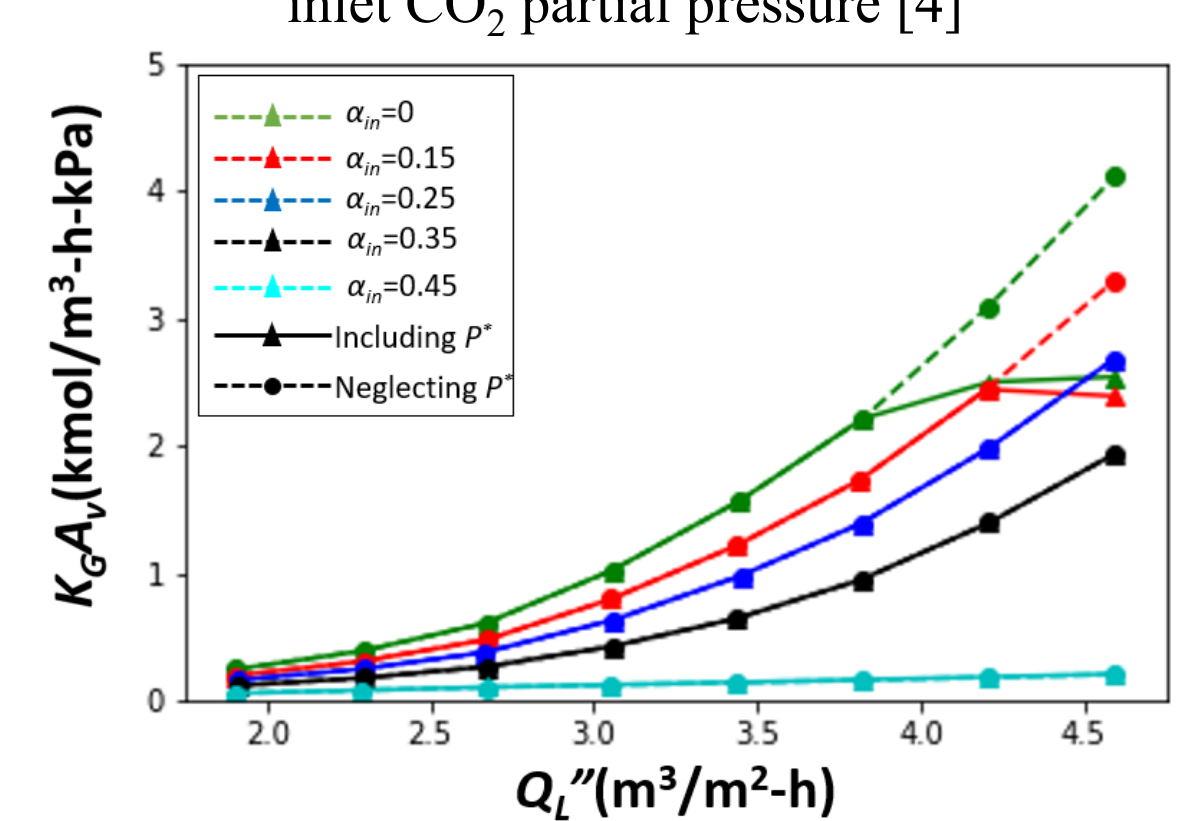


Figure 6: Model validation for variation in $K_G A_v$ with liquid flow rate [4]

Figure 7: Effect of P^* on the model predictions

- The purely analytical model predicted trends reasonably well.
- Model underpredicted and overpredicted K_GA_v at lower and higher liquid flow rates, respectively.
- The model's prediction after fitting is in good agreement with the experimental data.
- Model predictions can be used to estimate the system's performance for application with much lower partial pressure of CO_2 , for example, in the case of direct air capture.
- The model predictions can be used to extrapolate and estimate the ideal operating conditions.
- Enhanced capture for high liquid flow rate and low loading conditions cause the effect of P^* to be significant in that regime.
- Variation of parameters such as X_{CO_2} , α , K_GA_v , K_G , and A_v was studied along channel height.
- Optimal channel height can be estimated for any given operating conditions.

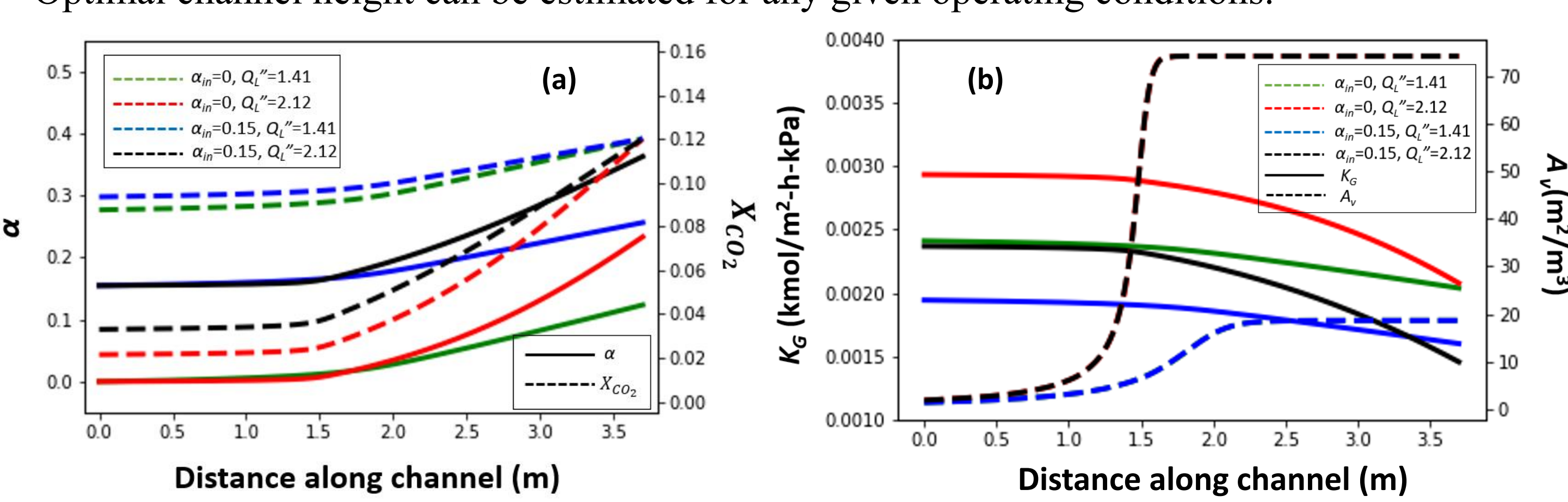
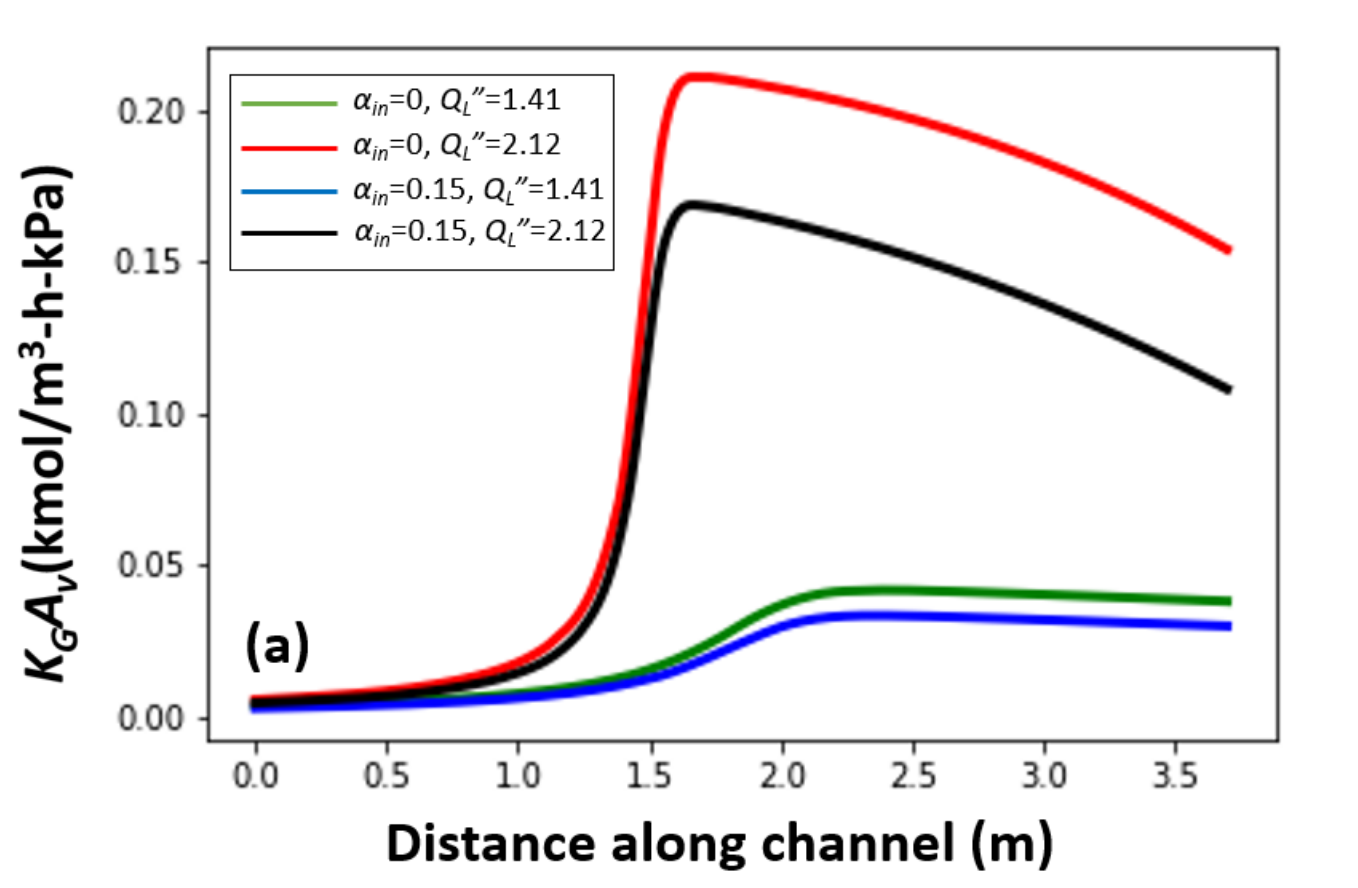


Figure 8: Variation of (a) α (solid line, left axis), X_{CO_2} (dashed line, right axis), and (b) K_G (solid line, left axis), A_{ν} (dashed line, right axis) along channel height using model validation results for [3]



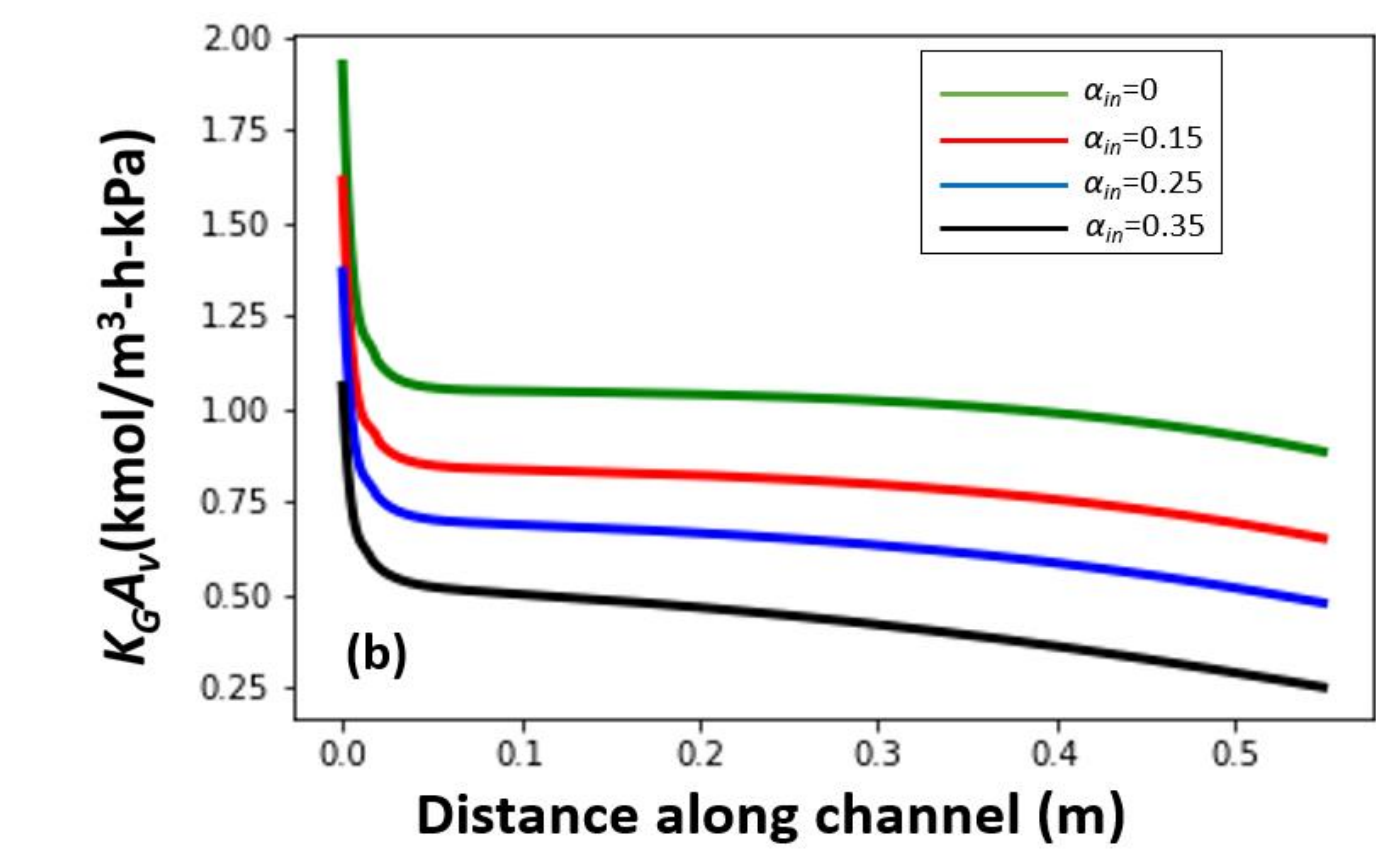


Figure 9: Variation of $K_G A_v$ along channel height using model validation results for (a) [3] and (b) [4]

CONCLUSIONS

- Effect of P^* is found to be significant only for high liquid flow rates, and low solvent loading.
- Model provides insights into performance of each section of the reactor independently.
- Model predictions can be used to get optimal working and design conditions.

REFERENCES

- [1] International Energy Agency (IEA).
- [2] Friedlingstein et. al., Global Carbon Budget 2021, Earth Syst. Sci. Data.
- [3] Y. Tamhankar et.al., "Spray absorption of CO2 into monoethanolamine: Mass transfer coefficients, dropsize, and planar surface area," Chem. Eng. Res. Des., vol. 104, pp. 376–389, 2015, doi: 10.1016/j.cherd.2015.08.012.
- [4] J. Kuntz and A. Aroonwilas, "Mass-transfer efficiency of a spray column for CO2 capture by MEA," in *Energy Procedia*, 2009, vol. 1, no. 1, pp. 205–209, doi: 10.1016/j.egypro.2009.01.029.

ACKNOWLEDGEMENTS

The authors would like to acknowledge fellow lab members Peter Mathews, Mark Hamalian, Karey Maynor, Yasmin Bibi, Palash Acharya and Aritra Kar for their continued support during the project. They would also like to acknowledge grant NSF CBET 1605789 for the financial support.